Measurement of the angle between jet axes in Pb-Pb collisions at $\sqrt{s_{NN}} = 5.02$ TeV

S. Acharya *et al.*[*]
(ALICE Collaboration)

(Received 23 July 2024; revised 6 October 2025; accepted 18 November 2025; published 13 April 2026)

This paper presents the first measurement of the angle between different jet axes (denoted as ΔR_{axis}) in Pb-Pb collisions. The measurement is carried out in the 0–10 % most-central events at $\sqrt{s_{NN}} = 5.02$ TeV. Jets are assembled by clustering charged particles at midrapidity using the anti-k_{T} algorithm with resolution parameters $R = 0.2$ and 0.4 and transverse momenta in the intervals $40 < p_{\text{T}}^{\text{ch jet}} < 140$ GeV/c and $80 < p_{\text{T}}^{\text{ch jet}} < 140$ GeV/c, respectively. Measurements at these low transverse momenta enhance the sensitivity to quark-gluon plasma (QGP) effects. A comparison to models implementing various mechanisms of jet energy loss in the QGP suggests that the observed narrowing of the Pb-Pb distribution relative to *pp* can be explained if quark-initiated jets are more likely to emerge from the medium than gluon-initiated jets. These new measurements disfavor intrajet p_{T} broadening as implemented in a simple model calculation with the Baier-Dokshitzer-Mueller-Peigne-Schiff formalism for energy loss in the QGP. The comparison of Pb-Pb and *pp* collisions shows sensitivity to the angular scale at which the QGP can resolve two independent splittings, favoring mechanisms that incorporate incoherent energy loss.

DOI: 10.1103/5bdl-cry6

I. INTRODUCTION

The strongly interacting, deconfined state of matter of our universe a few microseconds after the Big Bang can be recreated in ultrarelativistic heavy-ion collisions at the Large Hadron Collider (LHC) [1,2]. Studying the microscopic structure of this quark-gluon plasma (QGP) can elucidate the physics of many-body strongly coupled systems [3]. Because droplets of QGP created at colliders are small and short-lived, studying interactions within those droplets requires autogenerated probes. In this study, jets of energetic hadrons, which arise from high-momentum-transfer (hard) collisions between quarks and gluons (partons) in the incoming nuclei, are used. These hard-scattered particles produce showers of secondary partons, which give rise to jets of multiple correlated hadrons (see Fig. 1, left).

When traversing the QGP, jets interact with the medium, lose energy, and are modified relative to their structure in elementary (e.g., *ee* or *pp*) collisions [4–18]. Thus, measuring the substructure of jets can provide sensitivity to different scales within the jet modification process. The direction of a jet in rapidity (y) and azimuth (φ), referred to as the jet axis, is affected by transverse modification of the partonic shower, with varying sensitivity to soft radiation, depending on how the axis is defined [19].

This paper presents the first measurement in heavy-ion collisions of the angle between pairs of jet axes, ΔR_{axis} (see Fig. 1, right). This observable shows how well the QGP resolves the angular structure of the parton shower [19] and is defined as

$$\Delta R_{\text{axis}} \equiv \sqrt{(y_{\text{axis},1} - y_{\text{axis},2})^2 + (\varphi_{\text{axis},1} - \varphi_{\text{axis},2})^2}, \quad (1)$$

where $y_{\text{axis},i}$ and $\varphi_{\text{axis},i}$ are the rapidity and azimuthal coordinates of the axes, respectively. The axes considered in this analysis are as follows.

(i) Standard axis: coordinates in y-φ of the 4-vector resulting from clustering jets with the anti-k_{T} algorithm [20] using the E recombination scheme (two branches combined into one by adding their 4-momenta). In this case, all jet constituents including soft (low-transverse-momentum) and hard radiation contribute to the axis.

(ii) Soft Drop (SD) axis: coordinates in y-φ of the jet after soft wide-angle radiation is removed using the Soft Drop grooming procedure [21] with the Cambridge-Aachen (CA) reclustering algorithm [22,23]. The procedure stops when a splitting is found that satisfies the condition

$$\frac{\min(p_{\text{T},1}, p_{\text{T},2})}{p_{\text{T},1} + p_{\text{T},2}} > z_{\text{cut}} \left(\frac{\Delta R_{1,2}}{R}\right)^{\beta}, \quad (2)$$

where $p_{\text{T},i}$ are the transverse momenta of each of the two branches in the splitting, $\Delta R_{1,2}$ is the distance between them in the y-φ plane, R is the jet resolution parameter, and z_{cut} and β are user-set parameters.

[*]Full author list given at the end of the article.

Published by the American Physical Society under the terms of the Creative Commons Attribution 4.0 International license. Further distribution of this work must maintain attribution to the author(s) and the published article's title, journal citation, and DOI. Open access publication funded by CERN.

 ©2026 CERN, for the ALICE Collaboration

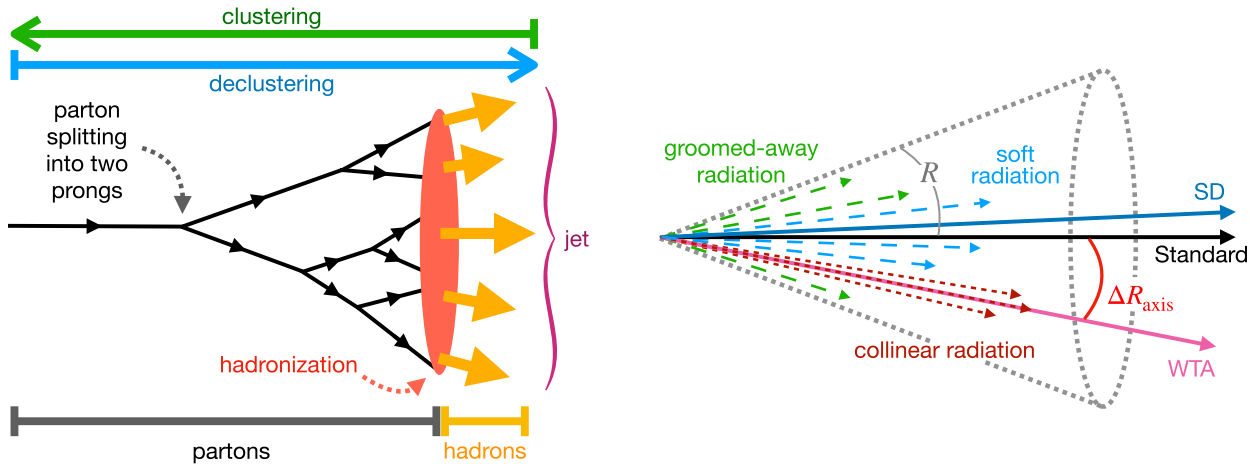


FIG. 1. Left: schematic of how energetic partons split or fragment into lower-energy prongs or branches of partons down to a scale in which hadrons emerge. An algorithm can then be run over final-state hadrons to cluster them into jets. An inverse declustering algorithm can be used to recursively explore the jet substructure. Right: schematic showing that different jet axes (solid arrows) can be selected from a jet to construct the ΔR_{axis} observable. The Standard axis (represented by a black arrow) is constrained by all the jet constituents (represented by dashed arrows). The soft drop (SD) axis (represented by a dark blue arrow) is determined by the particles left in the jet after grooming (blue and dark red arrows). Finally, the winner-takes-all (WTA) axis (represented by a pink arrow) tends to be aligned with the most energetic constituent.

(iii) Winner-Takes-All (WTA) axis: coordinates in y-φ of the jet after reclustering its constituents using the CA algorithm and the WTA p_{T} recombination scheme [24], which combines two jet branches into one by giving the merged branch the total p_{T} of the two sub-branches and the direction of the hardest sub-branch. The WTA axis is often consistent with the direction of the hardest constituent of the jet and is insensitive to soft radiation at the leading power of the observable [19].

Measurements of ΔR_{axis} are perturbatively calculable, but also sensitive to medium-induced effects; we examine sensitivity to such effects by studying jets of different p_{T} and radius parameter, R. An increase in the relative fraction of quark- vs gluon-initiated jets due to medium-induced radiative energy loss can narrow the angular distribution, while multiple scattering of the hard-scattered parton off medium partons can broaden it [25]. Reference [8] reported a net narrowing of the distribution in Pb-Pb collisions, quantitatively consistent with the former. This can be expected if the broadening was primarily in the wide-angle radiation that grooming removes from the jet. This is tested by looking for broadening effects in an ungroomed angular observable, such as the angle between the Standard and WTA axes. Increasing the grooming intensity and simultaneously varying the jet resolution parameter R can uncover medium-induced effects. Comparing experimental results with multiple models can help disentangle medium response and medium-induced large-angle radiation.

The medium resolution length, L_{res}, is a property of the QGP proportional to the inverse of its local temperature [26]. It characterizes the minimum separation distance at which two color charges within the same jet interact independently with the QGP. Certain jet substructure observables are sensitive to this scale [27]. In this analysis, the sensitivity of ΔR_{axis} to L_{res} is investigated.

The measured ΔR_{axis} distributions in pp collisions at $\sqrt{s} = 5.02$ TeV reported in Ref. [28] are used as the reference for QGP-induced effects reported here. Perturbative QCD calculations [19] were found to agree with the measurements in pp collisions within the experimental uncertainties, demonstrating good theoretical control of the observables.

II. EXPERIMENT

Data were collected in 2018 from Pb-Pb collisions at a center-of-mass energy per nucleon-nucleon pair of $\sqrt{s_{NN}} = 5.02$ TeV with the ALICE detector [2]. A detailed description of the detector and its performance can be found in Refs. [29,30]. A trigger based on the charged-particle multiplicity in the forward region [31] was used to select events in the 0–10 % centrality class [32,33]. The events were required to have a reconstructed primary vertex within ± 10 cm of the nominal interaction point in the longitudinal direction. Beam-induced background events were removed using two Zero Degree Calorimeters and pileup effects were removed by discarding events that contained multiple reconstructed vertices [4]. These selection criteria yield a data sample with 92 million events, corresponding to an integrated luminosity of approximately 0.12 nb^{-1}.

III. DATA ANALYSIS

Charged-particle tracks reconstructed in the Inner Tracking System (ITS) [34] and Time Projection Chamber (TPC) [35] used in the analysis were required to have a transverse momentum $p_{\text{T}} > 0.15$ GeV/c and a pseudorapidity $|\eta| < 0.9$. For details, see the Supplemental Material [36], including Refs. [2,5] therein. The detector performance was estimated

by propagating simulated events through a GEANT 3 [37] model of the ALICE detector. The transverse-momentum resolution $\sigma(p_{\mathrm{T}})/p_{\mathrm{T}}$ increases linearly from ≈1% at $p_{\mathrm{T}} = 1$ GeV/c to ≈4% at $p_{\mathrm{T}} = 50$ GeV/c [30]. The tracking efficiency rapidly increases from ≈65% at $p_{\mathrm{T}} = 0.15$ GeV/c to ≈85% at $p_{\mathrm{T}} = 1$ GeV/c, and remains above ≈75% at higher p_{T}. The large uncorrelated background from the underlying event (UE) [38] in high-multiplicity heavy-ion collisions is subtracted before jet finding, using the event-wide constituent subtraction procedure from Refs. [39,40]. The parameters used are $\alpha = 0$, $A_{\mathrm{g}} = 0.01$, and $\Delta R^{\mathrm{max}} = 0.1$ (0.25) when the track sample is used to cluster jets of $R = 0.2$ (0.4).

Tracks included in jet clustering are assigned the charged-pion mass. Charged-particle jets are clustered with the anti-k_{T} algorithm, the E recombination scheme, and resolution parameters $R = 0.2$ and 0.4, using FASTJET [41]. Jets containing a track with $p_{\mathrm{T}} > 100$ GeV/c and jets with their Standard axis not pointing inside the fiducial volume of the TPC ($|\eta_{\mathrm{jet}}| < 0.9 - R$) are discarded to minimize contamination by fake or partially reconstructed jets.

The measured distributions are unfolded to correct for detector effects as well as residual UE fluctuations using an iterative Bayesian procedure [42,43]. The procedure uses a 4D response matrix (RM) that captures the correspondence between ΔR_{axis} and jet transverse momentum ($p_{\mathrm{T}}^{\mathrm{ch\ jet}}$) at the generator and detector levels. The generator-level component of the RM is modeled using generated PYTHIA 8 [44] Monash 2013 [45] events. The detector-level component of the RM is modeled by propagating those events through a GEANT 3 [37] model of the ALICE detector and embedding the smeared events into measured Pb-Pb events.

Systematic uncertainties arise from the tracking inefficiency, unfolding procedure, unfolding model dependence, UE subtraction procedure, and residual effects from combinatorial jets. The tracking-inefficiency uncertainty is determined by repeating the analysis with an RM based on a track sample with 4% of all tracks randomly rejected. This number corresponds to the uncertainty in the tracking efficiency, determined by varying the track selection parameters and ITS-TPC matching criteria.

The unfolding-procedure uncertainty is determined by extending the lower and upper bounds of the $p_{\mathrm{T}}^{\mathrm{ch\ jet}}$ spectrum by 5 GeV/c, changing the detector-level ΔR_{axis} binning, changing the number of unfolding iterations, and scaling the prior distribution. The four categories of variations are carried out individually and combined into an unfolding uncertainty using their standard deviation. The uncertainty from the model dependence in the unfolding is determined by repeating the analysis with response matrices based on different event generators, including Herwig 7 [46] and JEWEL [47] with and without the inclusion of medium partons recoiling after interactions with the jet.

Potential bias introduced by the event-wide UE subtraction [39,40] is quantified as the maximum difference between the nominal result and the results obtained by repeating the procedure with parameters $\Delta R^{\mathrm{max}} = 0.05$ (0.1), which lead to an undersubtraction, and $\Delta R^{\mathrm{max}} = 0.5$ (0.7), which lead to an oversubtraction of the background, for jets of $R = 0.2$ (0.4). Deviations between the generator-level and unfolded distributions due to residual combinatorial jets are determined with a closure test. PYTHIA 8 events are embedded into background events with no jets and analyzed identically to the measured data. Deviations between the unfolded and PYTHIA 8 generator-level spectra are assigned as the uncertainty.

The systematic uncertainties are added in quadrature. The total systematic uncertainty is in the range 2–61% depending on ΔR_{axis} and $p_{\mathrm{T}}^{\mathrm{ch\ jet}}$. The large variation comes primarily from the background subtraction procedure at low $p_{\mathrm{T}}^{\mathrm{ch\ jet}}$ (where background effects are largest). It is small at low values of ΔR_{axis}, and smoothly grows in the tails of the distributions. The Supplemental Material [36] provides details.

The measured distributions are normalized to the total number of jets in a given $p_{\mathrm{T}}^{\mathrm{ch\ jet}}$ interval, N, which is equivalent to reporting the self-normalized cross section:

$$\frac{1}{N\left(p_{\mathrm{T}}^{\mathrm{ch\ jet}}\right)}\frac{\mathrm{d}N}{\mathrm{d}\Delta R_{\mathrm{axis}}}\left(p_{\mathrm{T}}^{\mathrm{ch\ jet}}\right) \equiv \frac{1}{\sigma\left(p_{\mathrm{T}}^{\mathrm{ch\ jet}}\right)}\frac{\mathrm{d}\sigma}{\mathrm{d}\Delta R_{\mathrm{axis}}}\left(p_{\mathrm{T}}^{\mathrm{ch\ jet}}\right). \quad (3)$$

This normalization choice causes the Pb-Pb/pp ratios to go above unity at low ΔR_{axis}. In an absolute cross-section measurement, the ratio would be below unity as a result of jet suppression in heavy-ion collisions. The suppression factor was measured in Ref. [48]. Thus, only the shape and not the absolute scale of the ΔR_{axis} spectra is reported.

IV. RESULTS AND DISCUSSION

The measured WTA-Standard distributions are shown in Fig. 2 for $R = 0.2$ jets in the $p_{\mathrm{T}}^{\mathrm{ch\ jet}}$ ranges [40,60] and [60,80] GeV/c. The top panels show ΔR_{axis} spectra from Pb-Pb and pp collisions. The vertical error bars represent the statistical uncertainties and the rectangles represent the total systematic uncertainties. The central and bottom panels show the Pb-Pb/pp ratio, with all uncertainties assumed uncorrelated and added in quadrature when calculating the ratio. The equivalent results for other $p_{\mathrm{T}}^{\mathrm{ch\ jet}}$ ranges, jet resolution parameters, and grooming settings are included in the Supplemental Material [36].

The data are compared with several jet quenching models. These models have different implementations of the microscopic properties of the medium, its evolution, and the jet-medium interaction. The JEWEL event generator [47] models the medium with a boost-invariant longitudinally expanding ideal quark-gluon gas [49]. Parameters from Ref. [50], which are adequate for the kinematics of this measurement, are used. The medium partons recoiling after interacting with jet constituents can be discarded from the event (recoils off) or allowed to hadronize together with the jet (recoils on). "MATTER+LBT" is from the JETSCAPE event generator [51,52], implementing an in-medium parton shower with interactions of high-virtuality (low-virtuality) partons with the medium described by the MATTER [53] (Linear Boltzmann Transport (LBT) [54]) model. The curve labeled "medium q/g" corresponds to a phenomenological model in which the only difference between the Pb-Pb and pp results comes from a modification of the fraction of quarks and gluons that initiate the jets [55,56], highlighting that these two jet populations lose energy differently in the medium. The

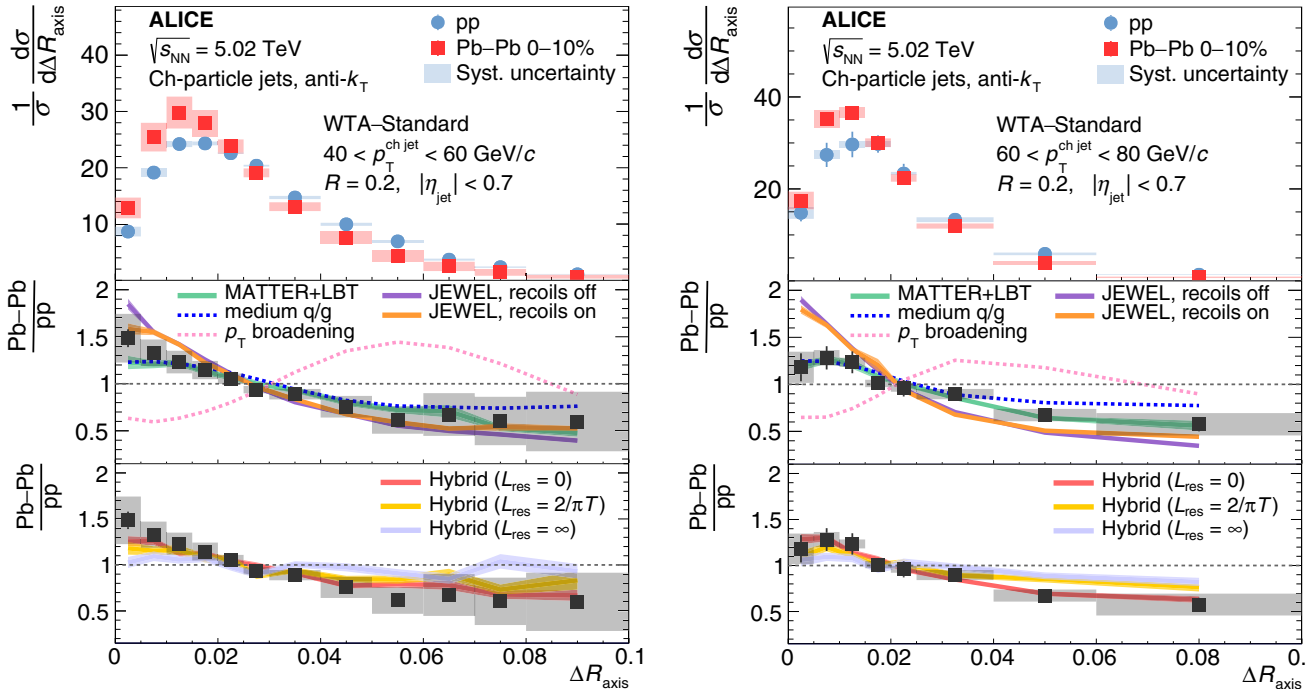


FIG. 2. Top: fully corrected Pb-Pb and pp $\Delta R_{axis}^{WTA\text{-}standard}$ distributions in the $p_T^{ch\ jet}$ intervals [40,60] (left), and [60,80] (right) GeV/c for jets of $R = 0.2$. The pp baseline is taken from Ref. [28]. Center and bottom: measured Pb-Pb/pp ratio in black, as well as predictions from a selection of jet quenching models.

"p_T broadening" calculation adds to the previous model a p_T broadening caused by incoherent multiple scatterings with the medium partons [25] following the Baier-Dokshitzer-Mueller-Peigne-Schiff (BDMPS) approach [57–59]. This calculation uses a mean-square momentum transfer coefficient between the jet and medium constituents, $\langle \hat{q}L \rangle = 5$ GeV^2. "Hybrid" is from the hybrid model [60], which describes the weakly coupled jet showering process using the Dokshitzer-Gribov-Lipatov-Altarelli-Parisi (DGLAP) formalism and the strongly coupled interaction between the jet constituents and medium partons via holographic calculations of energy loss based on AdS/CFT. The case $L_{res} = 0$ corresponds to fully incoherent energy loss, where the medium is able to resolve the splitting immediately after the parton fragments, resulting in higher energy loss [26]. The case $L_{res} = \infty$ corresponds to fully coherent energy loss, where the medium is not able to resolve splittings, and the energy loss is lower. The intermediate case, $L_{res} = 2/\pi T$, where T is the medium local temperature, is also included. All "Hybrid" curves include medium-response effects from Ref. [61] .

Figure 2 shows that the $R = 0.2$ distributions in Pb-Pb are narrower than those measured in pp collisions, as was also observed in Ref. [8]. The narrowing may be due to a selection bias, as jets selected using $p_T^{ch\ jet}$ (rather than the initial momentum before the jet-medium interactions, which is not accessible experimentally) tend to come from the surface and lose little energy in the QGP [62]. The data are also consistent with a quark-enhanced mixture of jets surviving the interaction with the medium relative to the vacuum case. This is expected since gluon-initiated jets couple more strongly to partons of the QGP and thus lose more energy [8,55,63]. The MATTER+LBT model generally describes the data for all considered kinematical regions.

Figure 3 compares jet axis difference distributions for 100–140 GeV/c jets with $R = 0.2$ and $R = 0.4$. We note that $R = 0.4$ jets have significantly larger systematic uncertainty due to larger background corrections; the systematics partially cancel in the ratio for $R = 0.2$ and $R = 0.4$. Consequently, model predictions are compared to this ratio. In contrast with $R = 0.2$, for larger R there are significant differences in JEWEL predictions with and without recoils for $R = 0.4$ jets. This is expected, as the medium response populates larger angles away from the Standard jet axis. The Hybrid model does not predict a significant effect on the jet axis from the medium response (see Ref. [36] for details). Comparison to other models in which the medium response can be turned on and off (e.g., the jet wake in Co-LBT [64,65]) could help clarify the sensitivity of ΔR_{axis} to the properties and magnitude of this effect. Narrowing of the distributions relative to those measured in pp collisions for jets of $R = 0.2$ is qualitatively predicted by all models except for "p_T broadening", which is calculated in a relatively simple formulation with a single value of $\hat{q}$. This tends to disagree with the hypothesis that intrajet p_T broadening manifests in the groomed radiation in previous measurements [8].

The data are closest to incoherent energy loss of jets in the Hybrid model ($L_{res} = 0$); the fully coherent case ($L_{res} = \infty$) predicts significantly less narrowing. Incoherent energy loss better reproduces the data than the intermediate case of $L_{res} = 2/\pi T$ even though holographic calculations of the

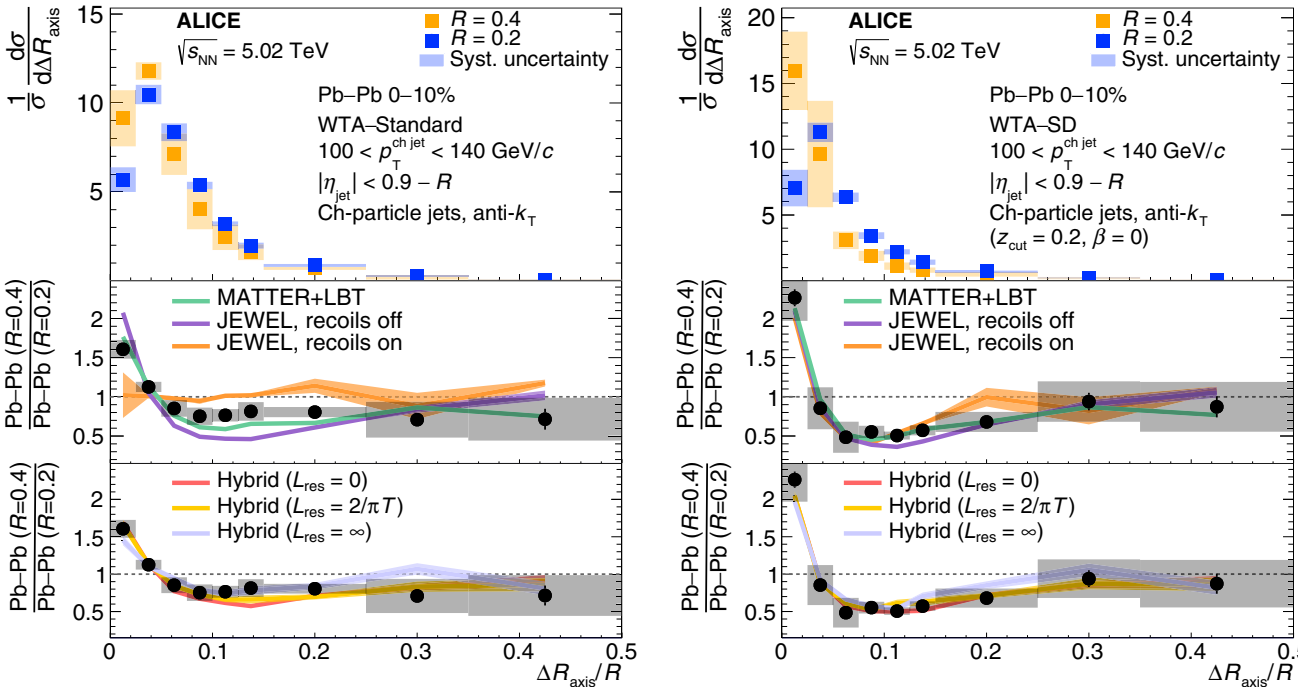


FIG. 3. Top: fully corrected Pb-Pb $\Delta R_{\text{axis}}^{\text{WTA-standard}}/R$ (left) and $\Delta R_{\text{axis}}^{\text{WTA-SD}}/R$ with ($z_{\text{cut}} = 0.2$, $\beta = 0$) (right) distributions in the $p_{\text{T}}^{\text{ch jet}}$ interval [100,140] GeV/c. Center and bottom: measured Pb-Pb($R = 0.4$)/Pb-Pb($R = 0.2$) ratio in black, as well as predictions from a selection of jet quenching models.

Debye screening length indicate that the intermediate case is closer to the true medium resolution scale [26].

The precision of the data at higher $p_{\text{T}}^{\text{ch jet}}$ is limited by the integrated luminosity of the pp dataset, which only allows for an extraction of the Pb-Pb/pp results up to 100 GeV/c. However, in heavy-ion collisions, larger $p_{\text{T}}^{\text{ch jet}}$ can be studied through the ratio of $(R = 0.4)/(R = 0.2)$ spectra, where the systematic uncertainties partially cancel. This kinematic range is also important for future comparisons with results from other experiments. The ratio is reported as a function of the jet angular scale $\Delta R_{\text{axis}}/R$ that, by construction, is independent of R [19]. Figure 3 shows the ratio for $p_{\text{T}}^{\text{ch jet}} \in [100, 140]$ GeV/c in ungroomed and groomed jets, together with theoretical predictions. The left-hand side shows that the Standard-WTA jet axis difference is narrower (closer to zero) for $R = 0.4$ than $R = 0.2$ jets. This implies, perhaps surprisingly, that jets including more wideangle radiation have their standard jet axis closer to the WTA axis. In groomed jets, the jet axis is even more aligned with the WTA axis. It should be noted, however, that the grooming here uses $\beta = 0$, which means that there is no angular weight and any soft branch can be groomed away.

The ungroomed WTA-Standard result is challenging to models, as can be seen in Fig. 3 (left). Grooming improves the agreement between the models and the data [see Fig. 3 (right)], suggesting that the ungroomed result captures significantly more of the nonperturbative aspects of jet quenching. The $(R = 0.4)/(R = 0.2)$ ratio of WTA-Standard jet axis is not very sensitive to L_{res} either with or without grooming. We have run PYTHIA 8 Monte Carlo to compare the ratios $R = 0.2/R = 0.4$ and we find that the WTA-Standard difference distribution does not change with the jet resolution parameter. In this, PYTHIA agrees with the measurement in Pb-Pb.

Figure 4 shows an intermediate grooming setting for 100–140 GeV/c jets. One can see by comparing $\Delta R_{\text{axis}}^{\text{WTA-standard}}$ to

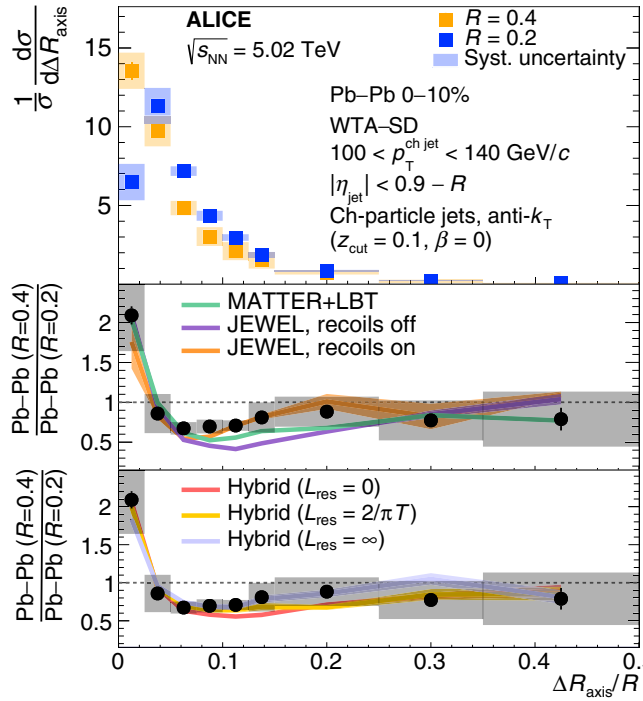


FIG. 4. Fully corrected WTA-SD ($z_{\text{cut}} = 0.1$, $\beta = 0$) distributions in the $100 < p_{\text{T}}^{\text{ch jet}} < 140$ GeV/c interval.

$\Delta R_{\text{axis}}^{\text{WTA-SD}}$ with different grooming settings (Fig. 4 vs Fig. 3, right) that once the softest branches are removed, further grooming does not substantially impact the jet axis. This was also seen in *pp* collisions, and shows that the Standard and SD axes are more aligned with each other than either of them is with the WTA axis. While the Standard axis is influenced by the soft wide-angle radiation present in $R = 0.4$ jets, grooming away more of the soft radiation does not further change the SD axis. This shows that once the softest particles are groomed away, the jet axis is dominated by the hard radiation. The models generally reproduce the intermediate grooming result, with the exception of JEWEL with recoils off. Stronger grooming improves the agreement, though some tension with the data remains. This reflects the importance of including medium response when calculating jet substructure in Pb-Pb collisions. PYTHIA studies agree with the general trend, but do not quantitatively reproduce the ratios. Given the medium effects, this is not surprising.

V. CONCLUSIONS

In summary, the first measurement of the angle between the WTA and Standard or Soft Drop groomed charged-particle jet axes in Pb-Pb collisions is reported. The measurement was carried out using the 0–10 % most-central collisions at $\sqrt{s_{NN}} = 5.02$ TeV with the ALICE detector and for $p_{\text{T}}^{\text{ch jet}} \in [40, 140]$ ([80,140]) GeV/c for jets of $R = 0.2$ (0.4).

Narrowing of the ΔR_{axis} distribution relative to the vacuum case is found. The narrowing may be explained if the Pb-Pb distribution is dominated by quark-initiated jets, since gluon-initiated jets are expected to interact more with the medium. This is consistent with the prediction from the "medium q/g" model. A selection bias causing apparent narrowing of the jet core should be reflected in all of the models which include energy loss. However, the distributions for ungroomed jets are not equally well described by the models, suggesting that the fate of large-angle prongs in the medium is important. The measurement disfavors intrajet p_{T} broadening, as implemented in Ref. [25] utilizing a single value of $\hat{q}$. The ΔR_{axis} observable is sensitive to the medium resolution length, favoring incoherent energy loss of jets, where the medium resolves a splitting immediately after it happens, regardless of the angular separation between the prongs.

For jets of 100–140 GeV p_T, $R = 0.4$ jet axes are more aligned with the WTA axis than those with $R = 0.2$. Grooming with $\beta = 0$ enhances this alignment. While grooming decreases the effects of medium response, fully reproducing both groomed and ungroomed jet axis differences requires including medium response in the models. Future measurements of ΔR_{axis} in photon- or Z-boson-tagged jets could provide a way to experimentally vary the fraction of quark- vs gluon-initiated jets and explore the relationship of the WTA axis to the initial parton direction.

ACKNOWLEDGMENTS

We gratefully acknowledge Felix Ringer, Daniel Pablos, and the JETSCAPE collaboration for providing theoretical predictions. We also acknowledge Xin-Nian Wang and Feng Yuan for fruitful discussions. The ALICE Collaboration would like to thank all its engineers and technicians for their invaluable contributions to the construction of the experiment and the CERN accelerator teams for the outstanding performance of the LHC complex. The ALICE Collaboration gratefully acknowledges the resources and support provided by all Grid centres and the Worldwide LHC Computing Grid (WLCG) collaboration. The ALICE Collaboration acknowledges the following funding agencies for their support in building and running the ALICE detector: A. I. Alikhanyan National Science Laboratory (Yerevan Physics Institute) Foundation (ANSL), State Committee of Science and World Federation of Scientists (WFS), Armenia; Austrian Academy of Sciences, Austrian Science Fund (FWF): [M 2467-N36] and Nationalstiftung für Forschung, Technologie und Entwicklung, Austria; Ministry of Communications and High Technologies, National Nuclear Research Center, Azerbaijan; Rede Nacional de Física de Altas Energias (Renafae), Financiadora de Estudos e Projetos (Finep), Fundação de Amparo à Pesquisa do Estado de São Paulo (FAPESP) and Universidade Federal do Rio Grande do Sul (UFRGS), Brazil; Bulgarian Ministry of Education and Science, within the National Roadmap for Research Infrastructures 2020-2027 (object CERN), Bulgaria; Ministry of Education of China (MOEC), Ministry of Science & Technology of China (MSTC) and National Natural Science Foundation of China (NSFC), China; Ministry of Science and Education and Croatian Science Foundation, Croatia; Centro de Aplicaciones Tecnológicas y Desarrollo Nuclear (CEADEN), Cubaenergía, Cuba; Ministry of Education, Youth and Sports of the Czech Republic, Czech Republic; The Danish Council for Independent Research | Natural Sciences, the VILLUM FONDEN and Danish National Research Foundation (DNRF), Denmark; Helsinki Institute of Physics (HIP), Finland; Commissariat à l'Energie Atomique (CEA) and Institut National de Physique Nucléaire et de Physique des Particules (IN2P3) and Centre National de la Recherche Scientifique (CNRS), France; Bundesministerium für Forschung, Technologie und Raumfahrt (BMFTR) and GSI Helmholtzzentrum für Schwerionenforschung GmbH, Germany; General Secretariat for Research and Technology, Ministry of Education, Research and Religions, Greece; National Research, Development and Innovation Office, Hungary; Department of Atomic Energy Government of India (DAE), Department of Science and Technology, Government of India (DST), University Grants Commission, Government of India (UGC) and Council of Scientific and Industrial Research (CSIR), India; National Research and Innovation Agency - BRIN, Indonesia; Istituto Nazionale di Fisica Nucleare (INFN), Italy; Japanese Ministry of Education, Culture, Sports, Science and Technology (MEXT) and Japan Society for the Promotion of Science (JSPS) KAKENHI, Japan; Consejo Nacional de Ciencia (CONACYT) y Tecnología, through Fondo de Cooperación Internacional en Ciencia y Tecnología (FONCICYT) and Dirección General de Asuntos del Personal Academico (DGAPA), Mexico; Nederlandse Organisatie voor Wetenschappelijk Onderzoek (NWO), Netherlands; The Research Council of

Norway, Norway; Commission on Science and Technology for Sustainable Development in the South (COMSATS), Pakistan; Pontificia Universidad Católica del Perú, Peru; Ministry of Science and Higher Education, National Science Centre and WUT ID-UB, Poland; Korea Institute of Science and Technology Information and National Research Foundation of Korea (NRF), Republic of Korea; Ministry of Education and Scientific Research, Institute of Atomic Physics, Ministry of Research and Innovation and Institute of Atomic Physics and Universitatea Nationala de Stiinta si Tehnologie Politehnica Bucuresti, Romania; Ministerstvo skolstva, vyskumu, vyvoja a mladeze SR, Slovakia; National Research Foundation of South Africa, South Africa; Swedish Research Council (VR) and Knut & Alice Wallenberg Foundation (KAW), Sweden; European Organization for Nuclear Research, Switzerland; Suranaree University of Technology (SUT), National Science and Technology Development Agency (NSTDA) and National Science, Research and Innovation Fund (NSRF via PMU-B B05F650021), Thailand; Turkish Energy, Nuclear and Mineral Research Agency (TENMAK), Turkey; National Academy of Sciences of Ukraine, Ukraine; Science and Technology Facilities Council (STFC), United Kingdom; National Science Foundation of the United States of America (NSF) and United States Department of Energy, Office of Nuclear Physics (DOE NP), United States of America. In addition, individual groups or members have received support from: Czech Science Foundation (Grant No. 23-07499S), Czech Republic; European Research Council (Grant No. 950692), European Union; Strong 2020 - Horizon 2020 (Grant Nos. 824093), European Union; ICSC - Centro Nazionale di Ricerca in High Performance Computing, Big Data and Quantum Computing, European Union - NextGenerationEU; Academy of Finland (Center of Excellence in Quark Matter) (Grants No. 346327 and No. 346328), Finland; Deutsche Forschungs Gemeinschaft (DFG, German Research Foundation) "Neutrinos and Dark Matter in Astro- and Particle Physics" (Grant No. SFB 1258), Germany; Programa de Apoyos para la Superación del Personal Académico, UNAM, Mexico.

DATA AVAILABILITY

This manuscript has associated data in a HEPData repository at [66].

[1] W. Busza, K. Rajagopal, and W. van der Schee, Heavy ion collisions: The big picture, and the big questions, Annu. Rev. Nucl. Part. Sci. **68**, 339 (2018).

[2] S. Acharya *et al.* (ALICE Collaboration), The ALICE experiment–A journey through QCD, Eur. Phys. J. C **84**, 813 (2024).

[3] B. V. Jacak and B. Müller, The exploration of hot nuclear matter, Science **337**, 310 (2012).

[4] S. Acharya *et al.* (ALICE Collaboration), Measurements of inclusive jet spectra in *pp* and central Pb-Pb collisions at $\sqrt{s_{NN}} =$ 5.02 TeV, Phys. Rev. C **101**, 034911 (2020).

[5] M. Aaboud *et al.* (ATLAS Collaboration), Measurement of the nuclear modification factor for inclusive jets in Pb+Pb collisions at $\sqrt{s_{\rm NN}} = 5.02$ TeV with the ATLAS detector, Phys. Lett. B **790**, 108 (2019).

[6] A. M. Sirunyan *et al.* (CMS Collaboration), First measurement of large area jet transverse momentum spectra in heavy-ion collisions, J. High Energy Phys. 05 (2021) 284.

[7] J. Adam *et al.* (STAR Collaboration), Measurement of inclusive charged-particle jet production in Au + Au collisions at $\sqrt{s_{NN}} = 200$ GeV, Phys. Rev. C **102**, 054913 (2020).

[8] S. Acharya *et al.* (ALICE Collaboration), Measurement of the groomed jet radius and momentum splitting fraction in *pp* and Pb-Pb collisions at $\sqrt{s_{NN}} = 5.02$ TeV, Phys. Rev. Lett. **128**, 102001 (2022).

[9] S. Acharya *et al.* (ALICE Collaboration), Medium modification of the shape of small-radius jets in central Pb-Pb collisions at $\sqrt{s_{\rm NN}} = 2.76$ TeV, J. High Energy Phys. 10 (2018) 139.

[10] M. Aaboud *et al.* (ATLAS Collaboration), Measurement of jet fragmentation in Pb+Pb and *pp* collisions at $\sqrt{s_{NN}} = 5.02$ TeV with the ATLAS detector, Phys. Rev. C **98**, 024908 (2018).

[11] M. Aaboud *et al.* (ATLAS Collaboration), Comparison of fragmentation functions for jets dominated by light quarks and gluons from *pp* and Pb+Pb collisions in ATLAS, Phys. Rev. Lett. **123**, 042001 (2019).

[12] G. Aad *et al.* (ATLAS Collaboration), Measurement of suppression of large-radius jets and its dependence on substructure in Pb+Pb collisions at $\sqrt{s_{NN}} = 5.02$ TeV with the ATLAS detector, Phys. Rev. Lett. **131**, 172301 (2023).

[13] S. Chatrchyan *et al.* (CMS Collaboration), Measurement of jet fragmentation in PbPb and *pp* collisions at $\sqrt{s_{NN}} = 2.76$ TeV, Phys. Rev. C **90**, 024908 (2014).

[14] A. M. Sirunyan *et al.* (CMS Collaboration), Observation of medium-induced modifications of jet fragmentation in Pb-Pb collisions at $\sqrt{s_{NN}} = 5.02$ TeV using isolated photon-tagged jets, Phys. Rev. Lett. **121**, 242301 (2018).

[15] A. M. Sirunyan *et al.* (CMS Collaboration), Measurement of the splitting function in *pp* and Pb-Pb collisions at $\sqrt{s_{NN}} =$ 5.02 TeV, Phys. Rev. Lett. **120**, 142302 (2018).

[16] A. M. Sirunyan *et al.* (CMS Collaboration), Measurement of the groomed jet mass in Pb-Pb and *pp* collisions at $\sqrt{s_{NN}} =$ 5.02 TeV, J. High Energy Phys. 10 (2018) 161.

[17] J. Adam *et al.* (ALICE Collaboration), Measurement of jet quenching with semi-inclusive hadron-jet distributions in central Pb-Pb collisions at $\sqrt{s_{NN}} = 2.76$ TeV, J. High Energy Phys. 09 (2015) 170.

[18] L. Adamczyk *et al.* (STAR Collaboration), Measurements of jet quenching with semi-inclusive hadron jet distributions in Au+Au collisions at $\sqrt{s_{NN}} = 200$ GeV, Phys. Rev. C **96**, 024905 (2017).

[19] P. Cal, D. Neill, F. Ringer, and W. J. Waalewijn, Calculating the angle between jet axes, J. High Energy Phys. 04 (2020) 211.

[20] M. Cacciari, G. P. Salam, and G. Soyez, The anti-k_t jet clustering algorithm, J. High Energy Phys. 04 (2008) 063.

[21] A. J. Larkoski, S. Marzani, G. Soyez, and J. Thaler, Soft Drop, J. High Energy Phys. 05 (2014) 146.

[22] Y. L. Dokshitzer, G. D. Leder, S. Moretti, and B. R. Webber, Better jet clustering algorithms, J. High Energy Phys. 08 (1997) 001.

[23] M. Wobisch and T. Wengler, Hadronization corrections to jet cross-sections in deep inelastic scattering, arXiv:hep-ph/9907280.

[24] D. Bertolini, T. Chan, and J. Thaler, Jet observables without jet algorithms, J. High Energy Phys. 04 (2014) 013.

[25] F. Ringer, B.-W. Xiao, and F. Yuan, Can we observe jet P_T-broadening in heavy-ion collisions at the LHC? Phys. Lett. B **808**, 135634 (2020).

[26] Z. Hulcher, D. Pablos, and K. Rajagopal, Resolution effects in the hybrid strong/weak coupling model, J. High Energy Phys. 03 (2018) 010.

[27] J. Casalderrey-Solana, J. G. Milhano, D. Pablos, and K. Rajagopal, Modification of Jet substructure in heavy ion collisions as a probe of the resolution length of quark-gluon plasma, J. High Energy Phys. 01 (2020) 044.

[28] S. Acharya *et al.* (ALICE Collaboration), Measurement of the angle between jet axes in *pp* collisions at $\sqrt{s} = 5.02$ TeV, J. High Energy Phys. 07 (2023) 201.

[29] K. Aamodt *et al.* (ALICE Collaboration), The ALICE experiment at the CERN LHC, J. Instrum. **3**, S08002 (2008).

[30] B. Abelev *et al.* (ALICE Collaboration), Performance of the ALICE Experiment at the CERN LHC, Int. J. Mod. Phys. A **29**, 1430044 (2014).

[31] E. Abbas *et al.* (ALICE Collaboration), Performance of the ALICE VZERO system, J. Instrum. **8**, P10016 (2013).

[32] B. Abelev *et al.* (ALICE Collaboration), Centrality determination of Pb-Pb collisions at $\sqrt{s_{NN}} = 2.76$ TeV with ALICE, Phys. Rev. C **88**, 044909 (2013).

[33] ALICE Collaboration, Centrality determination in heavy ion collisions, ALICE-PUBLIC-2018-011 (2018), https://cds.cern.ch/record/2636623

[34] K. Aamodt *et al.* (ALICE Collaboration), Alignment of the ALICE Inner Tracking System with cosmic-ray tracks, J. Instrum. **5**, P03003 (2010).

[35] J. Alme *et al.*, The ALICE TPC, a large 3-dimensional tracking device with fast readout for ultra-high multiplicity events, Nucl. Instrum. Methods Phys. Res., Sect. A **622**, 316 (2010).

[36] See Supplemental Material at http://link.aps.org/supplemental/10.1103/5bdl-cry6 for additional information and results.

[37] R. Brun, F. Bruyant, M. Maire, A. C. McPherson, and P. Zanarini, *GEANT 3: user's guide Geant 3.10, Geant 3.11; rev. version* (CERN, Geneva, 1987), https://cds.cern.ch/record/1119728

[38] B. Abelev *et al.* (ALICE Collaboration), Measurement of event background fluctuations for charged particle jet reconstruction in Pb–Pb collisions at $\sqrt{s_{NN}} = 2.76$ TeV, J. High Energy Phys. 03 (2012) 053.

[39] P. Berta, M. Spousta, D. W. Miller, and R. Leitner, Particle-level pileup subtraction for jets and jet shapes, J. High Energy Phys. 06 (2014) 092.

[40] P. Berta, L. Masetti, D. W. Miller, and M. Spousta, Pileup and underlying event mitigation with iterative constituent subtraction, J. High Energy Phys. 08 (2019) 175.

[41] M. Cacciari, G. P. Salam, and G. Soyez, FastJet user manual, Eur. Phys. J. C **72**, 1896 (2012).

[42] G. D'Agostini, A multidimensional unfolding method based on Bayes' theorem, Nucl. Instrum. Methods Phys. Res., Sect. A **362**, 487 (1995).

[43] G. D'Agostini, Improved iterative Bayesian unfolding, arXiv:1010.0632.

[44] T. Sjöstrand, S. Ask, J. R. Christiansen, R. Corke, N. Desai, P. Ilten, S. Mrenna, S. Prestel, C. O. Rasmussen, and P. Z. Skands, An introduction to PYTHIA 8.2, Comput. Phys. Commun. **191**, 159 (2015).

[45] P. Skands, S. Carrazza, and J. Rojo, Tuning PYTHIA 8.1: the Monash 2013 Tune, Eur. Phys. J. C **74**, 3024 (2014).

[46] S. Gieseke, C. Rohr, and A. Siodmok, Colour reconnections in Herwig, Eur. Phys. J. C **72**, 2225 (2012).

[47] K. C. Zapp, JEWEL 2.0.0: directions for use, Eur. Phys. J. C **74**, 2762 (2014).

[48] S. Acharya *et al.* (ALICE Collaboration), Measurement of the radius dependence of charged-particle jet suppression in Pb-Pb collisions at $\sqrt{s_{NN}} = 5.02$ TeV, Phys. Lett. B **849**, 138412 (2024).

[49] K. C. Zapp, F. Krauss, and U. A. Wiedemann, A perturbative framework for jet quenching, J. High Energy Phys. 03 (2013) 080.

[50] R. Kunnawalkam Elayavalli and K. C. Zapp, Medium response in JEWEL and its impact on jet shape observables in heavy ion collisions, J. High Energy Phys. 07 (2017) 141.

[51] J. H. Putschke *et al.*, The JETSCAPE framework, arXiv:1903.07706.

[52] A. Kumar *et al.* (JETSCAPE Collaboration), Inclusive Jet and hadron suppression in a multi-stage approach, Phys. Rev. C **107**, 034911 (2023).

[53] A. Majumder, Incorporating space-time within medium-modified jet event generators, Phys. Rev. C **88**, 014909 (2013).

[54] Y. He, T. Luo, X.-N. Wang, and Y. Zhu, Linear Boltzmann transport for jet propagation in the quark-gluon plasma: Elastic processes and medium recoil, Phys. Rev. C **91**, 054908 (2015); Erratum: Linear Boltzmann transport for jet propagation in the quark-gluon plasma: Elastic processes and medium recoil [Phys. Rev. C **91**, 054908 (2015)], **97**, 019902(E) (2018).

[55] J.-W. Qiu, F. Ringer, N. Sato, and P. Zurita, Factorization of jet cross sections in heavy-ion collisions, Phys. Rev. Lett. **122**, 252301 (2019).

[56] J.-W. Qiu, F. Ringer, N. Sato, and P. Zurita, QCD factorization and universality of jet cross sections in heavy-ion collisions, Nucl. Phys. A **1005**, 121853 (2021).

[57] R. Baier, Y. L. Dokshitzer, A. H. Mueller, S. Peigne, and D. Schiff, Radiative energy loss of high-energy quarks and gluons in a finite volume quark–gluon plasma, Nucl. Phys. B **483**, 291 (1997).

[58] R. Baier, Y. L. Dokshitzer, A. H. Mueller, S. Peigne, and D. Schiff, Radiative energy loss and p(T) broadening of high-energy partons in nuclei, Nucl. Phys. B **484**, 265 (1997).

[59] R. Baier, Y. L. Dokshitzer, A. H. Mueller, and D. Schiff, Medium induced radiative energy loss: Equivalence between the BDMPS and Zakharov formalisms, Nucl. Phys. B **531**, 403 (1998).

[60] J. Casalderrey-Solana, D. C. Gulhan, J. G. Milhano, D. Pablos, and K. Rajagopal, A hybrid strong/weak coupling approach to jet quenching, J. High Energy Phys. 10 (2014) 019;

Erratum to: A hybrid strong/weak coupling approach to jet quenching, 09 (2015) 175.

[61] J. Casalderrey-Solana, D. C. Gulhan, J. G. Milhano, D. Pablos, and K. Rajagopal, Angular structure of jet quenching within a hybrid strong/weak coupling model, J. High Energy Phys. 03 (2017) 135.

[62] J. Brewer, Q. Brodsky, and K. Rajagopal, Disentangling jet modification in jet simulations and in Z jet data, J. High Energy Phys. 02 (2022) 175.

[63] M. Spousta and B. Cole, Interpreting single jet measurements in Pb + Pb collisions at the LHC, Eur. Phys. J. C **76**, 50 (2016).

[64] W. Chen, S. Cao, T. Luo, L.-G. Pang, and X.-N. Wang, Effects of jet-induced medium excitation in γ-hadron correlation in A+A collisions, Phys. Lett. B **777**, 86 (2018).

[65] W. Zhao, W. Ke, W. Chen, T. Luo, and X.-N. Wang, From hydrodynamics to jet quenching, coalescence, and hadron cascade: A coupled approach to solving the $R_{AA} \otimes v_2$ puzzle, Phys. Rev. Lett. **128**, 022302 (2022).

[66] ALICE Collaboration, HEPData repository (2026), https://www.hepdata.net/record/ins2648610.

S. Acharya,[126] D. Adamová,[87] A. Adler,[70] G. Aglieri Rinella,[32] M. Agnello,[29] N. Agrawal,[51] Z. Ahammed,[134] S. Ahmad,[15] S. U. Ahn,[71] I. Ahuja,[36] A. Akindinov,[140] M. Al-Turany,[98] D. Aleksandrov,[140] B. Alessandro,[56] H. M. Alfanda,[6] R. Alfaro Molina,[67] B. Ali,[15] A. Alici,[25,a] N. Alizadehvandchali,[115] A. Alkin,[32] J. Alme,[20] G. Alocco,[52] T. Alt,[64] I. Altsybeev,[140] J. R. Alvarado,[44] M. N. Anaam,[6] C. Andrei,[45] A. Andronic,[125] V. Anguelov,[95] F. Antinori,[54] P. Antonioli,[51] N. Apadula,[74] L. Aphecetche,[103] H. Appelshäuser,[64] C. Arata,[73] S. Arcelli,[25] M. Aresti,[52] R. Arnaldi,[56] J. G. M. C. A. Arneiro,[110] I. C. Arsene,[19] M. Arslandok,[137] A. Augustinus,[32] R. Averbeck,[98] M. D. Azmi,[15] A. Badalà,[53] J. Bae,[104] Y. W. Baek,[40] X. Bai,[119] R. Bailhache,[64] Y. Bailung,[48] A. Balbino,[29] A. Baldisseri,[129] B. Balis,[2] D. Banerjee,[4] Z. Banoo,[92] R. Barbera,[26] F. Barile,[31] L. Barioglio,[96] M. Barlou,[79] G. G. Barnaföldi,[46] L. S. Barnby,[86] V. Barret,[126] L. Barreto,[110] C. Bartels,[118] K. Barth,[32] E. Bartsch,[64] N. Bastid,[126] S. Basu,[75,a] G. Batigne,[103] D. Battistini,[96] B. Batyunya,[141] D. Bauri,[47] J. L. Bazo Alba,[102] I. G. Bearden,[84] C. Beattie,[137] P. Becht,[98] D. Behera,[48] I. Belikov,[128] A. D. C. Bell Hechavarria,[125] F. Bellini,[25] R. Bellwied,[115] S. Belokurova,[140] G. Bencedi,[46] S. Beole,[24] Y. Berdnikov,[140] A. Berdnikova,[95] L. Bergmann,[95] M. G. Besoiu,[63] L. Betev,[32] P. P. Bhaduri,[134] A. Bhasin,[92] M. A. Bhat,[4] B. Bhattacharjee,[41] L. Bianchi,[24] N. Bianchi,[49] J. Bielčík,[34] J. Bielčíková,[87] J. Biernat,[107] A. P. Bigot,[128] A. Bilandzic,[96] G. Biro,[46] S. Biswas,[4] N. Bize,[103] J. T. Blair,[108] D. Blau,[140] M. B. Blidaru,[98] N. Bluhme,[38] C. Blume,[64] G. Boca,[21,55] F. Bock,[88] T. Bodova,[20] A. Bogdanov,[140] S. Boi,[22] J. Bok,[58] L. Boldizsár,[46] M. Bombara,[36] P. M. Bond,[32] G. Bonomi,[133,55] H. Borel,[129] A. Borissov,[140] A. G. Borquez Carcamo,[95] H. Bossi,[137] E. Botta,[24] Y. E. M. Bouziani,[64] L. Bratrud,[64] P. Braun-Munzinger,[98] M. Bregant,[110] M. Broz,[34] G. E. Bruno,[97,31] M. D. Buckland,[23] D. Budnikov,[140] H. Buesching,[64] S. Bufalino,[29] P. Buhler,[76] Z. Buthelezi,[68,122] A. Bylinkin,[20] S. A. Bysiak,[107] M. Cai,[6] H. Caines,[137] A. Caliva,[28] E. Calvo Villar,[102] J. M. M. Camacho,[109] P. Camerini,[23] F. D. M. Canedo,[110] S. L. Cantway,[137] M. Carabas,[113] A. A. Carballo,[32] F. Carnesecchi,[32] R. Caron,[127] L. A. D. Carvalho,[110] J. Castillo Castellanos,[129] F. Catalano,[32,24] C. Ceballos Sanchez,[141] I. Chakaberia,[74] P. Chakraborty,[47] S. Chandra,[134] S. Chapeland,[32] M. Chartier,[118] S. Chattopadhyay,[134] S. Chattopadhyay,[100] T. Cheng,[98,6] C. Cheshkov,[127] B. Cheynis,[127] V. Chibante Barroso,[32] D. D. Chinellato,[111] E. S. Chizzali,[96,b] J. Cho,[58] S. Cho,[58] P. Chochula,[32] S. Choudhury,[100] P. Christakoglou,[85] C. H. Christensen,[84] P. Christiansen,[75] T. Chujo,[124] M. Ciacco,[29] C. Cicalo,[52] F. Cindolo,[51] M. R. Ciupek,[98] G. Clai,[51,c] F. Colamaria,[50] J. S. Colburn,[101] D. Colella,[97,31] M. Colocci,[25] M. Concas,[56,138] G. Conesa Balbastre,[73] Z. Conesa del Valle,[130] G. Contin,[23] J. G. Contreras,[34] M. L. Coquet,[129] T. M. Cormier,[88,a] P. Cortese,[132,56] M. R. Cosentino,[112] F. Costa,[32] S. Costanza,[21,55] C. Cot,[130] J. Crkovská,[95] P. Crochet,[126] R. Cruz-Torres,[74] P. Cui,[6] A. Dainese,[54] M. C. Danisch,[95] A. Danu,[63] P. Das,[81] P. Das,[4] S. Das,[4] A. R. Dash,[125] S. Dash,[47] A. De Caro,[28] G. de Cataldo,[50] J. de Cuveland,[38] A. De Falco,[22] D. De Gruttola,[28] N. De Marco,[56] C. De Martin,[23] S. De Pasquale,[28] R. Deb,[133] S. Deb,[48] K. R. Deja,[135] R. Del Grande,[96] L. Dello Stritto,[28] W. Deng,[6] P. Dhankher,[18] D. Di Bari,[31] A. Di Mauro,[32] B. Diab,[129] R. A. Diaz,[141,7] T. Dietel,[114] Y. Ding,[6] R. Divià,[32] D. U. Dixit,[18] Ø. Djuvsland,[20] U. Dmitrieva,[140] A. Dobrin,[63] B. Dönigus,[64] J. M. Dubinski,[135] A. Dubla,[98] S. Dudi,[91] P. Dupieux,[126] M. Durkac,[106] N. Dzalaiova,[12] T. M. Eder,[125] R. J. Ehlers,[74] F. Eisenhut,[64] D. Elia,[50] B. Erazmus,[103] F. Ercolessi,[25] F. Erhardt,[90] M. R. Ersdal,[20] B. Espagnon,[130] G. Eulisse,[32] D. Evans,[101] S. Evdokimov,[140] L. Fabbietti,[96] M. Faggin,[27] J. Faivre,[73] F. Fan,[6] W. Fan,[74] T. Fang,[6] A. Fantoni,[49] M. Fasel,[88] P. Fecchio,[29] A. Feliciello,[56] G. Feofilov,[140] A. Fernández Téllez,[44] L. Ferrandi,[110] M. B. Ferrer,[32] A. Ferrero,[129] C. Ferrero,[56,d] A. Ferretti,[24] V. J. G. Feuillard,[95] D. Finogeev,[140] F. M. Fionda,[52] F. Flor,[115] A. N. Flores,[108] S. Foertsch,[68] I. Fokin,[95] S. Fokin,[140] E. Fragiacomo,[57] E. Frajna,[46] U. Fuchs,[32] N. Funicello,[28] C. Furget,[73] A. Furs,[140] T. Fusayasu,[99] J. J. Gaardhøje,[84] M. Gagliardi,[24] A. M. Gago,[102] C. D. Galvan,[109] D. R. Gangadharan,[115] P. Ganoti,[79] C. Garabatos,[98] T. García Chávez,[44] E. Garcia-Solis,[9] C. Gargiulo,[32] K. Garner,[125] P. Gasik,[98] A. Gautam,[117] M. B. Gay Ducati,[66] M. Germain,[103] A. Ghimouz,[124] C. Ghosh,[134] M. Giacalone,[51,25] P. Giubellino,[98,56] P. Giubilato,[27] A. M. C. Glaenzer,[129] P. Glässel,[95] E. Glimos,[121]

D. J. Q. Goh,[77] V. Gonzalez,[136] M. Gorgon,[2] K. Goswami,[48] S. Gotovac,[33] V. Grabski,[67] L. K. Graczykowski,[135] E. Grecka,[87] A. Grelli,[59] C. Grigoras,[32] V. Grigoriev,[140] S. Grigoryan,[141,1] F. Grosa,[32] J. F. Grosse-Oetringhaus,[32] R. Grosso,[98] D. Grund,[34] G. G. Guardiano,[111] R. Guernane,[73] M. Guilbaud,[103] K. Gulbrandsen,[84] T. Gündem,[64] T. Gunji,[123] W. Guo,[6] A. Gupta,[92] R. Gupta,[92] R. Gupta,[48] K. Gwizdziel,[135] L. Gyulai,[46] M. K. Habib,[98] C. Hadjidakis,[130] F. U. Haider,[92] H. Hamagaki,[77] A. Hamdi,[74] M. Hamid,[6] Y. Han,[138] B. G. Hanley,[136] R. Hannigan,[108] J. Hansen,[75] M. R. Haque,[135] J. W. Harris,[137] A. Harton,[9] H. Hassan,[88] D. Hatzifotiadou,[51] P. Hauer,[42] L. B. Havener,[137] S. T. Heckel,[96] E. Hellbär,[98] H. Helstrup,[37] M. Hemmer,[64] T. Herman,[34] G. Herrera Corral,[8] F. Herrmann,[125] S. Herrmann,[127] K. F. Hetland,[37] B. Heybeck,[64] H. Hillemanns,[32] B. Hippolyte,[128] F. W. Hoffmann,[70] B. Hofman,[59] B. Hohlweger,[85] G. H. Hong,[138] A. Horzyk,[2] Y. Hou,[6] P. Hristov,[32] C. Hughes,[121] P. Huhn,[64] L. M. Huhta,[116] T. J. Humanic,[89] V. Humlova,[34] A. Hutson,[115] D. Hutter,[38] R. Ilkaev,[140] H. Ilyas,[13] M. Inaba,[124] G. M. Innocenti,[32] M. Ippolitov,[140] A. Isakov,[87] T. Isidori,[117] M. S. Islam,[100] M. Ivanov,[12] M. Ivanov,[98] V. Ivanov,[140] K. E. Iversen,[75] M. Jablonski,[2] B. Jacak,[74] N. Jacazio,[25] P. M. Jacobs,[74] S. Jadlovska,[106] J. Jadlovsky,[106] S. Jaelani,[83] C. Jahnke,[111] M. J. Jakubowska,[135] D. M. Janik,[34] M. A. Janik,[135] T. Janson,[70] M. Jercic,[90] S. Ji,[16] S. Jia,[10] A. A. P. Jimenez,[65] F. Jonas,[88,125] J. M. Jowett,[32,98] J. Jung,[64] M. Jung,[64] A. Junique,[32] A. Jusko,[101] J. Kaewjai,[105] P. Kalinak,[60] A. S. Kalteyer,[98] A. Kalweit,[32] V. Kaplin,[140] A. Karasu Uysal,[72] D. Karatovic,[90] O. Karavichev,[140] T. Karavicheva,[140] P. Karczmarczyk,[135] E. Karpechev,[140] M. J. Karwowska,[32,135] U. Kebschull,[70] R. Keidel,[139] D. L. D. Keijdener,[59] M. Keil,[32] B. Ketzer,[42] S. S. Khade,[48] A. M. Khan,[119,6] S. Khan,[15] A. Khanzadeev,[140] Y. Kharlov,[140] A. Khatun,[117] A. Khuntia,[107] M. B. Kidson,[114] B. Kileng,[37] B. Kim,[104] C. Kim,[16] D. J. Kim,[116] E. J. Kim,[69] J. Kim,[138] J. S. Kim,[40] J. Kim,[58] J. Kim,[69] M. Kim,[18] S. Kim,[17] T. Kim,[138] K. Kimura,[93] O. A. M. Kirjamäki,[43] S. Kirsch,[64] I. Kisel,[38] S. Kiselev,[140] A. Kisiel,[135] J. P. Kitowski,[2] J. L. Klay,[5] J. Klein,[32] S. Klein,[74] C. Klein-Bösing,[125] M. Kleiner,[64] T. Klemenz,[96] A. Kluge,[32] A. G. Knospe,[115,e] C. Kobdaj,[105] T. Kollegger,[98] A. Kondratyev,[141] N. Kondratyeva,[140] E. Kondratyuk,[140] J. Konig,[64] S. A. Konigstorfer,[96] P. J. Konopka,[32] G. Kornakov,[135] M. Korwieser,[96] S. D. Koryciak,[2] A. Kotliarov,[87] V. Kovalenko,[140] M. Kowalski,[107] V. Kozhuharov,[35] I. Králik,[60] A. Kravčáková,[36] L. Krcal,[32,38] M. Krivda,[101,60] F. Krizek,[87] K. Krizkova Gajdosova,[32] M. Kroesen,[95] M. Krüger,[64] E. Kryshen,[140] V. Kučera,[58] C. Kuhn,[128] P. G. Kuijer,[85,a] T. Kumaoka,[124] D. Kumar,[134] L. Kumar,[91] N. Kumar,[91] S. Kumar,[31] S. Kundu,[32] P. Kurashvili,[80] A. Kurepin,[140] A. B. Kurepin,[140] A. Kuryakin,[140] S. Kushpil,[87] J. Kvapil,[101] M. J. Kweon,[58] Y. Kwon,[138] S. L. La Pointe,[38] P. La Rocca,[26] A. Lakrathok,[105] M. Lamanna,[32] A. R. Landou,[73] R. Langoy,[120] P. Larionov,[32] E. Laudi,[32] L. Lautner,[32,96] R. Lavicka,[76] R. Lea,[133,55] H. Lee,[104] I. Legrand,[45] G. Legras,[125] J. Lehrbach,[38] T. M. Lelek,[2] R. C. Lemmon,[86,a] I. León Monzón,[109] M. M. Lesch,[96] E. D. Lesser,[18] P. Lévai,[46] X. Li,[10] X. L. Li,[6] J. Lien,[120] R. Lietava,[101] I. Likmeta,[115] B. Lim,[24] S. H. Lim,[16] V. Lindenstruth,[38] A. Lindner,[45] C. Lippmann,[98] A. Liu,[18] D. H. Liu,[6] J. Liu,[118] G. S. S. Liveraro,[111] I. M. Lofnes,[20] C. Loizides,[88] S. Lokos,[107] J. Lömker,[59] P. Loncar,[33] J. A. Lopez,[95] X. Lopez,[126] E. López Torres,[7] P. Lu,[98,119] J. R. Luhder,[125] M. Lunardon,[27] G. Luparello,[57] Y. G. Ma,[39] M. Mager,[32] M. Mahlein,[96] A. Maire,[128] M. V. Makariev,[35] M. Malaev,[140] G. Malfattore,[25] N. M. Malik,[92] Q. W. Malik,[19] S. K. Malik,[92] L. Malinina,[141,a] D. Mallick,[81] N. Mallick,[48] G. Mandaglio,[30,53] S. K. Mandal,[80] V. Manko,[140] F. Manso,[126] V. Manzari,[50] Y. Mao,[6] R. W. Marcjan,[2] G. V. Margagliotti,[23] A. Margotti,[51] A. Marín,[98] C. Markert,[108] P. Martinengo,[32] M. I. Martínez,[44] G. Martínez García,[103] M. P. P. Martins,[110] S. Masciocchi,[98] M. Masera,[24] A. Masoni,[52] L. Massacrier,[130] A. Mastroserio,[131,50] O. Matonoha,[75] S. Mattiazzo,[27] P. F. T. Matuoka,[110] A. Matyja,[107] C. Mayer,[107] A. L. Mazuecos,[32] F. Mazzaschi,[24] M. Mazzilli,[32] J. E. Mdhluli,[122] A. F. Mechler,[64] Y. Melikyan,[43,140] A. Menchaca-Rocha,[67] E. Meninno,[76] A. S. Menon,[115] M. Meres,[12] S. Mhlanga,[114,68] Y. Miake,[124] L. Micheletti,[32] L. C. Migliorin,[127] D. L. Mihaylov,[96] K. Mikhaylov,[141,140] A. N. Mishra,[46] D. Miśkowiec,[98] A. Modak,[4] A. P. Mohanty,[59] B. Mohanty,[81] M. Mohisin Khan,[15,f] M. A. Molander,[43] Z. Moravcova,[84] C. Mordasini,[96] D. A. Moreira De Godoy,[125] I. Morozov,[140] A. Morsch,[32] T. Mrnjavac,[32] V. Muccifora,[49] S. Muhuri,[134] J. D. Mulligan,[74] A. Mulliri,[22] M. G. Munhoz,[110] R. H. Munzer,[64] H. Murakami,[123] S. Murray,[114] L. Musa,[32] J. Musinsky,[60] J. W. Myrcha,[135] B. Naik,[122] A. I. Nambrath,[18] B. K. Nandi,[47] R. Nania,[51] E. Nappi,[50] A. F. Nassirpour,[17,75] A. Nath,[95] C. Nattrass,[121] M. N. Naydenov,[35] A. Neagu,[19] A. Negru,[113] L. Nellen,[65] G. Neskovic,[38] N. Nicassio,[31] B. S. Nielsen,[84] E. G. Nielsen,[84] S. Nikolaev,[140] S. Nikulin,[140] V. Nikulin,[140] F. Noferini,[51] S. Noh,[11] P. Nomokonov,[141] J. Norman,[118] N. Novitzky,[124] P. Nowakowski,[135] A. Nyanin,[140] J. Nystrand,[20] M. Ogino,[77] A. Ohlson,[75] V. A. Okorokov,[140] J. Oleniacz,[135] A. C. Oliveira Da Silva,[121] M. H. Oliver,[137] A. Onnerstad,[116] C. Oppedisano,[56] A. Ortiz Velasquez,[65] J. Otwinowski,[107] M. Oya,[93] K. Oyama,[77] Y. Pachmayer,[95] S. Padhan,[47] D. Pagano,[133,55] G. Paić,[65] S. Paisano-Guzmán,[44] A. Palasciano,[50] S. Panebianco,[129] H. Park,[124] H. Park,[104] J. Park,[58] J. E. Parkkila,[32] R. N. Patra,[92] B. Paul,[22] H. Pei,[6] T. Peitzmann,[59] X. Peng,[6] M. Pennisi,[24] D. Peresunko,[140] G. M. Perez,[7] S. Perrin,[129] Y. Pestov,[140] V. Petrov,[140] M. Petrovici,[45] R. P. Pezzi,[103,66] S. Piano,[57] M. Pikna,[12] P. Pillot,[103] O. Pinazza,[51,32] L. Pinsky,[115] C. Pinto,[96] S. Pisano,[49] M. Płoskoń,[74] M. Planinic,[90] F. Pliquett,[64] M. G. Poghosyan,[88] B. Polichtchouk,[140] S. Politano,[29] N. Poljak,[90] A. Pop,[45] S. Porteboeuf-Houssais,[126] V. Pozdniakov,[141,a] I. Y. Pozos,[44] K. K. Pradhan,[48] S. K. Prasad,[4] S. Prasad,[48]

R. Preghenella,[51] F. Prino,[56] C. A. Pruneau,[136] I. Pshenichnov,[140] M. Puccio,[32] S. Pucillo,[24] Z. Pugelova,[106] S. Qiu,[85] L. Quaglia,[24] R. E. Quishpe,[115] S. Ragoni,[14] A. Rakotozafindrabe,[129] L. Ramello,[132,56] F. Rami,[128] T. A. Rancien,[73] M. Rasa,[26] S. S. Räsänen,[43] R. Rath,[51] M. P. Rauch,[20] I. Ravasenga,[85] K. F. Read,[88,121] C. Reckziegel,[112] A. R. Redelbach,[38] K. Redlich,[80,g] C. A. Reetz,[98] H. D. Regules-Medel,[44] A. Rehman,[20] F. Reidt,[32] H. A. Reme-Ness,[37] Z. Rescakova,[36] K. Reygers,[95] A. Riabov,[140] V. Riabov,[140] R. Ricci,[28] M. Richter,[19] A. A. Riedel,[96] W. Riegler,[32] C. Ristea,[63] M. V. Rodriguez,[32] M. Rodríguez Cahuantzi,[44] S. A. Rodríguez Ramírez,[44] K. Røed,[19] R. Rogalev,[140] E. Rogochaya,[141] T. S. Rogoschinski,[64] D. Rohr,[32] D. Röhrich,[20] P. F. Rojas,[44] S. Rojas Torres,[34] P. S. Rokita,[135] G. Romanenko,[141] F. Ronchetti,[49] A. Rosano,[30,53] E. D. Rosas,[65] K. Roslon,[135] A. Rossi,[54] A. Roy,[48] S. Roy,[47] N. Rubini,[25] D. Ruggiano,[135] R. Rui,[23] P. G. Russek,[2] R. Russo,[85] A. Rustamov,[82] E. Ryabinkin,[140] Y. Ryabov,[140] A. Rybicki,[107] H. Rytkonen,[116] J. Ryu,[16] W. Rzesa,[135] R. Sadek,[103] S. Sadhu,[31] S. Sadovsky,[140] J. Saetre,[20] K. Šafařík,[34,a] P. Saha,[41] S. K. Saha,[4] S. Saha,[81] B. Sahoo,[47] B. Sahoo,[48] R. Sahoo,[48] S. Sahoo,[61] D. Sahu,[48] P. K. Sahu,[61] J. Saini,[134] K. Sajdakova,[36] S. Sakai,[124] M. P. Salvan,[98] S. Sambyal,[92] I. Sanna,[32,96] T. B. Saramela,[110] D. Sarkar,[136] N. Sarkar,[134] P. Sarma,[41] V. Sarritzu,[22] V. M. Sarti,[96] M. H. P. Sas,[137] J. Schambach,[88] H. S. Scheid,[64] C. Schiaua,[45] R. Schicker,[95] A. Schmah,[95] C. Schmidt,[98] H. R. Schmidt,[94] M. O. Schmidt,[32] M. Schmidt,[94] N. V. Schmidt,[88] A. R. Schmier,[121] R. Schotter,[128] A. Schröter,[38] J. Schukraft,[32] K. Schwarz,[98] K. Schweda,[98] G. Scioli,[25] E. Scomparin,[56] J. E. Seger,[14] Y. Sekiguchi,[123] D. Sekihata,[123] I. Selyuzhenkov,[98] S. Senyukov,[128] J. J. Seo,[58] D. Serebryakov,[140] L. Šerkšnytė,[96] A. Sevcenco,[63] T. J. Shaba,[68] A. Shabetai,[103] R. Shahoyan,[32] A. Shangaraev,[140] A. Sharma,[91] B. Sharma,[92] D. Sharma,[47] H. Sharma,[54,107] M. Sharma,[92] S. Sharma,[77] S. Sharma,[92] U. Sharma,[92] A. Shatat,[130] O. Sheibani,[115] K. Shigaki,[93] M. Shimomura,[78] J. Shin,[11,a] S. Shirinkin,[140] Q. Shou,[39] Y. Sibiriak,[140] S. Siddhanta,[52] T. Siemiarczuk,[80] T. F. Silva,[110] D. Silvermyr,[75] T. Simantathammakul,[105] R. Simeonov,[35] B. Singh,[92] B. Singh,[96] K. Singh,[48] R. Singh,[81] R. Singh,[92] R. Singh,[48] S. Singh,[15] V. K. Singh,[134] V. Singhal,[134] T. Sinha,[100] B. Sitar,[12] M. Sitta,[132,56] T. B. Skaali,[19] G. Skorodumovs,[95] M. Slupecki,[43] N. Smirnov,[137] R. J. M. Snellings,[59] E. H. Solheim,[19] J. Song,[115,16] A. Songmoolnak,[105] C. Sonnabend,[32,98] F. Soramel,[27] A. B. Soto-Hernandez,[89] R. Spijkers,[85] I. Sputowska,[107] J. Staa,[75] J. Stachel,[95] I. Stan,[63] P. J. Steffanic,[121] S. F. Stiefelmaier,[95] D. Stocco,[103] I. Storehaug,[19] P. Stratmann,[125] S. Strazzi,[25] C. P. Stylianidis,[85] A. A. P. Suaide,[110] C. Suire,[130] M. Sukhanov,[140] M. Suljic,[32] R. Sultanov,[140] V. Sumberia,[92] S. Sumowidagdo,[83] S. Swain,[61] I. Szarka,[12] M. Szymkowski,[135] S. F. Taghavi,[96] G. Taillepied,[98] J. Takahashi,[111] G. J. Tambave,[81] S. Tang,[6] Z. Tang,[119] J. D. Tapia Takaki,[117] N. Tapus,[113] L. A. Tarasovicova,[125] M. G. Tarzila,[45] G. F. Tassielli,[31] A. Tauro,[32] G. Tejeda Muñoz,[44] A. Telesca,[32] L. Terlizzi,[24] C. Terrevoli,[115] S. Thakur,[4] D. Thomas,[108] A. Tikhonov,[140] A. R. Timmins,[115] M. Tkacik,[106] T. Tkacik,[106] A. Toia,[64] R. Tokumoto,[93] N. Topilskaya,[140] M. Toppi,[49] T. Tork,[130] A. G. Torres Ramos,[31] A. Trifiró,[30,53] A. S. Triolo,[32,30,53] S. Tripathy,[51] T. Tripathy,[47] S. Trogolo,[32] V. Trubnikov,[3] W. H. Trzaska,[116] T. P. Trzcinski,[135] A. Tumkin,[140] R. Turrisi,[54] T. S. Tveter,[19] K. Ullaland,[20] B. Ulukutlu,[96] A. Uras,[127] M. Urioni,[55,133] G. L. Usai,[22] M. Vala,[36] N. Valle,[21] L. V. R. van Doremalen,[59] M. van Leeuwen,[85] C. A. van Veen,[95] R. J. G. van Weelden,[85] P. Vande Vyvre,[32] D. Varga,[46] Z. Varga,[46] M. Vasileiou,[79] A. Vasiliev,[140,a] O. Vázquez Doce,[49] O. Vazquez Rueda,[115] V. Vechernin,[140] E. Vercellin,[24] S. Vergara Limón,[44] L. Vermunt,[98] R. Vértesi,[46] M. Verweij,[59] L. Vickovic,[33] Z. Vilakazi,[122] O. Villalobos Baillie,[101] A. Villani,[23] G. Vino,[50] A. Vinogradov,[140] T. Virgili,[28] M. M. O. Virta,[116] V. Vislavicius,[75] A. Vodopyanov,[141] B. Volkel,[32] M. A. Völkl,[95] K. Voloshin,[140] S. A. Voloshin,[136] G. Volpe,[31] B. von Haller,[32] I. Vorobyev,[96] N. Vozniuk,[140] J. Vrláková,[36] J. Wan,[39] C. Wang,[39] D. Wang,[39] Y. Wang,[39] A. Wegrzynek,[32] F. T. Weiglhofer,[38] S. C. Wenzel,[32] J. P. Wessels,[125] J. Wiechula,[64] J. Wikne,[19] G. Wilk,[80] J. Wilkinson,[98] G. A. Willems,[125] B. Windelband,[95] M. Winn,[129] J. R. Wright,[108] W. Wu,[39] Y. Wu,[119] L. Xu,[6] R. Xu,[6] A. Yadav,[42] A. K. Yadav,[134] S. Yalcin,[72] Y. Yamaguchi,[93] S. Yang,[20] S. Yano,[93] Z. Yin,[6] I.-K. Yoo,[16] J. H. Yoon,[58] H. Yu,[11] S. Yuan,[20] A. Yuncu,[95] V. Zaccolo,[23] C. Zampolli,[32] F. Zanone,[95] N. Zardoshti,[32] A. Zarochentsev,[140] P. Závada,[62] N. Zaviyalov,[140] M. Zhalov,[140] B. Zhang,[6] L. Zhang,[39] M. Zhang,[6] S. Zhang,[39] X. Zhang,[6] Y. Zhang,[119] Z. Zhang,[6] M. Zhao,[10] V. Zherebchevskii,[140] Y. Zhi,[10] D. Zhou,[6] Y. Zhou,[84] J. Zhu,[98,6] Y. Zhu,[6] S. C. Zugravel,[56] and N. Zurlo[133,55]

(ALICE Collaboration)

[1]*A.I. Alikhanyan National Science Laboratory (Yerevan Physics Institute) Foundation, Yerevan, Armenia*
[2]*AGH University of Krakow, Cracow, Poland*
[3]*Bogolyubov Institute for Theoretical Physics, National Academy of Sciences of Ukraine, Kyiv, Ukraine*
[4]*Bose Institute, Department of Physics and Centre for Astroparticle Physics and Space Science (CAPSS), Kolkata, India*
[5]*California Polytechnic State University, San Luis Obispo, California, USA*
[6]*Central China Normal University, Wuhan, China*
[7]*Centro de Aplicaciones Tecnológicas y Desarrollo Nuclear (CEADEN), Havana, Cuba*
[8]*Centro de Investigación y de Estudios Avanzados (CINVESTAV), Mexico City and Mérida, Mexico*

[9]*Chicago State University, Chicago, Illinois, USA*
[10]*China Nuclear Data Center, China Institute of Atomic Energy, Beijing, China*
[11]*Chungbuk National University, Cheongju, Republic of Korea*
[12]*Comenius University Bratislava, Faculty of Mathematics, Physics and Informatics, Bratislava, Slovak Republic*
[13]*COMSATS University Islamabad, Islamabad, Pakistan*
[14]*Creighton University, Omaha, Nebraska, USA*
[15]*Department of Physics, Aligarh Muslim University, Aligarh, India*
[16]*Department of Physics, Pusan National University, Pusan, Republic of Korea*
[17]*Department of Physics, Sejong University, Seoul, Republic of Korea*
[18]*Department of Physics, University of California, Berkeley, California, USA*
[19]*Department of Physics, University of Oslo, Oslo, Norway*
[20]*Department of Physics and Technology, University of Bergen, Bergen, Norway*
[21]*Dipartimento di Fisica, Università di Pavia, Pavia, Italy*
[22]*Dipartimento di Fisica dell'Università and Sezione INFN, Cagliari, Italy*
[23]*Dipartimento di Fisica dell'Università and Sezione INFN, Trieste, Italy*
[24]*Dipartimento di Fisica dell'Università and Sezione INFN, Turin, Italy*
[25]*Dipartimento di Fisica e Astronomia dell'Università and Sezione INFN, Bologna, Italy*
[26]*Dipartimento di Fisica e Astronomia dell'Università and Sezione INFN, Catania, Italy*
[27]*Dipartimento di Fisica e Astronomia dell'Università and Sezione INFN, Padova, Italy*
[28]*Dipartimento di Fisica 'E.R. Caianiello' dell'Università and Gruppo Collegato INFN, Salerno, Italy*
[29]*Dipartimento DISAT del Politecnico and Sezione INFN, Turin, Italy*
[30]*University of Cagliari, Università di Messina, Messina, Italy*
[31]*Dipartimento Interateneo di Fisica 'M. Merlin' and Sezione INFN, Bari, Italy*
[32]*European Organization for Nuclear Research (CERN), Geneva, Switzerland*
[33]*Faculty of Electrical Engineering, Mechanical Engineering and Naval Architecture, University of Split, Split, Croatia*
[34]*Faculty of Nuclear Sciences and Physical Engineering, Czech Technical University in Prague, Prague, Czech Republic*
[35]*Faculty of Physics, Sofia University, Sofia, Bulgaria*
[36]*Faculty of Science, P.J. Šafárik University, Košice, Slovak Republic*
[37]*Faculty of Technology, Environmental and Social Sciences, Bergen, Norway*
[38]*Frankfurt Institute for Advanced Studies, Johann Wolfgang Goethe-Universität Frankfurt, Frankfurt, Germany*
[39]*Fudan University, Shanghai, China*
[40]*Gangneung-Wonju National University, Gangneung, Republic of Korea*
[41]*Gauhati University, Department of Physics, Guwahati, India*
[42]*Helmholtz-Institut für Strahlen- und Kernphysik, Rheinische Friedrich-Wilhelms-Universität Bonn, Bonn, Germany*
[43]*Helsinki Institute of Physics (HIP), Helsinki, Finland*
[44]*High Energy Physics Group, Universidad Autónoma de Puebla, Puebla, Mexico*
[45]*Horia Hulubei National Institute of Physics and Nuclear Engineering, Bucharest, Romania*
[46]*HUN-REN Wigner Research Centre for Physics, Budapest, Hungary*
[47]*Indian Institute of Technology Bombay (IIT), Mumbai, India*
[48]*Indian Institute of Technology Indore, Indore, India*
[49]*INFN, Laboratori Nazionali di Frascati, Frascati, Italy*
[50]*INFN, Sezione di Bari, Bari, Italy*
[51]*INFN, Sezione di Bologna, Bologna, Italy*
[52]*INFN, Sezione di Cagliari, Cagliari, Italy*
[53]*INFN, Sezione di Catania, Catania, Italy*
[54]*INFN, Sezione di Padova, Padova, Italy*
[55]*INFN, Sezione di Pavia, Pavia, Italy*
[56]*INFN, Sezione di Torino, Turin, Italy*
[57]*INFN, Sezione di Trieste, Trieste, Italy*
[58]*Inha University, Incheon, Republic of Korea*
[59]*Institute for Gravitational and Subatomic Physics (GRASP), Utrecht University/Nikhef, Utrecht, Netherlands*
[60]*Institute of Experimental Physics, Slovak Academy of Sciences, Košice, Slovak Republic*
[61]*Institute of Physics, Homi Bhabha National Institute, Bhubaneswar, India*
[62]*Institute of Physics of the Czech Academy of Sciences, Prague, Czech Republic*
[63]*Institute of Space Science (ISS), Bucharest, Romania*
[64]*Institut für Kernphysik, Johann Wolfgang Goethe-Universität Frankfurt, Frankfurt, Germany*
[65]*Instituto de Ciencias Nucleares, Universidad Nacional Autónoma de México, Mexico City, Mexico*
[66]*Instituto de Física, Universidade Federal do Rio Grande do Sul (UFRGS), Porto Alegre, Brazil*
[67]*Instituto de Física, Universidad Nacional Autónoma de México, Mexico City, Mexico*

[68] *iThemba LABS, National Research Foundation, Somerset West, South Africa*
[69] *Jeonbuk National University, Jeonju, Republic of Korea*
[70] *Johann-Wolfgang-Goethe Universität Frankfurt Institut für Informatik, Fachbereich Informatik und Mathematik, Frankfurt, Germany*
[71] *Korea Institute of Science and Technology Information, Daejeon, Republic of Korea*
[72] *KTO Karatay University, Konya, Turkey*
[73] *Laboratoire de Physique Subatomique et de Cosmologie, Université Grenoble-Alpes, CNRS-IN2P3, Grenoble, France*
[74] *Lawrence Berkeley National Laboratory, Berkeley, California, USA*
[75] *Lund University Department of Physics, Division of Particle Physics, Lund, Sweden*
[76] *Marietta Blau Institute, Vienna, Austria*
[77] *Nagasaki Institute of Applied Science, Nagasaki, Japan*
[78] *Nara Women's University (NWU), Nara, Japan*
[79] *National and Kapodistrian University of Athens, School of Science, Department of Physics, Athens, Greece*
[80] *National Centre for Nuclear Research, Warsaw, Poland*
[81] *National Institute of Science Education and Research, Homi Bhabha National Institute, Jatni, India*
[82] *National Nuclear Research Center, Baku, Azerbaijan*
[83] *National Research and Innovation Agency - BRIN, Jakarta, Indonesia*
[84] *Niels Bohr Institute, University of Copenhagen, Copenhagen, Denmark*
[85] *Nikhef, National institute for subatomic physics, Amsterdam, Netherlands*
[86] *Nuclear Physics Group, STFC Daresbury Laboratory, Daresbury, United Kingdom*
[87] *Nuclear Physics Institute of the Czech Academy of Sciences, Husinec-Řež, Czech Republic*
[88] *Oak Ridge National Laboratory, Oak Ridge, Tennessee, USA*
[89] *Ohio State University, Columbus, Ohio, USA*
[90] *Physics department, Faculty of science, University of Zagreb, Zagreb, Croatia*
[91] *Physics Department, Panjab University, Chandigarh, India*
[92] *Physics Department, University of Jammu, Jammu, India*
[93] *Physics Program and International Institute for Sustainability with Knotted Chiral Meta Matter (WPI-SKCM^2), Hiroshima University, Hiroshima, Japan*
[94] *Physikalisches Institut, Eberhard-Karls-Universität Tübingen, Tübingen, Germany*
[95] *Physikalisches Institut, Ruprecht-Karls-Universität Heidelberg, Heidelberg, Germany*
[96] *Physik Department, Technische Universität München, Munich, Germany*
[97] *Politecnico di Bari and Sezione INFN, Bari, Italy*
[98] *Research Division and ExtreMe Matter Institute EMMI, GSI Helmholtzzentrum für Schwerionenforschung GmbH, Darmstadt, Germany*
[99] *Saga University, Saga, Japan*
[100] *Saha Institute of Nuclear Physics, Homi Bhabha National Institute, Kolkata, India*
[101] *School of Physics and Astronomy, University of Birmingham, Birmingham, United Kingdom*
[102] *Sección Física, Departamento de Ciencias, Pontificia Universidad Católica del Perú, Lima, Peru*
[103] *SUBATECH, IMT Atlantique, Nantes Université, CNRS-IN2P3, Nantes, France*
[104] *Sungkyunkwan University, Suwon City, Republic of Korea*
[105] *Suranaree University of Technology, Nakhon Ratchasima, Thailand*
[106] *Technical University of Košice, Košice, Slovak Republic*
[107] *The Henryk Niewodniczanski Institute of Nuclear Physics, Polish Academy of Sciences, Cracow, Poland*
[108] *The University of Texas at Austin, Austin, Texas, USA*
[109] *Universidad Autónoma de Sinaloa, Culiacán, Mexico*
[110] *Universidade de São Paulo (USP), São Paulo, Brazil*
[111] *Universidade Estadual de Campinas (UNICAMP), Campinas, Brazil*
[112] *Universidade Federal do ABC, Santo Andre, Brazil*
[113] *Universitatea Nationala de Stiinta si Tehnologie Politehnica Bucuresti, Bucharest, Romania*
[114] *University of Cape Town, Cape Town, South Africa*
[115] *University of Houston, Houston, Texas, USA*
[116] *University of Jyväskylä, Jyväskylä, Finland*
[117] *University of Kansas, Lawrence, Kansas, USA*
[118] *University of Liverpool, Liverpool, United Kingdom*
[119] *University of Science and Technology of China, Hefei, China*
[120] *University of South-Eastern Norway, Kongsberg, Norway*
[121] *University of Tennessee, Knoxville, Tennessee, USA*
[122] *University of the Witwatersrand, Johannesburg, South Africa*
[123] *University of Tokyo, Tokyo, Japan*
[124] *University of Tsukuba, Tsukuba, Japan*
[125] *Universität Münster, Institut für Kernphysik, Münster, Germany*

[126] *Université Clermont Auvergne, CNRS/IN2P3, LPC, Clermont-Ferrand, France*
[127] *Université de Lyon, CNRS/IN2P3, Institut de Physique des 2 Infinis de Lyon, Lyon, France*
[128] *Université de Strasbourg, CNRS, IPHC UMR 7178, F-67000 Strasbourg, France, Strasbourg, France*
[129] *Université Paris-Saclay, Centre d'Etudes de Saclay (CEA), IRFU, Départment de Physique Nucléaire (DPhN), Saclay, France*
[130] *Université Paris-Saclay, CNRS/IN2P3, IJCLab, Orsay, France*
[131] *Università degli Studi di Foggia, Foggia, Italy*
[132] *Università del Piemonte Orientale, Vercelli, Italy*
[133] *Università di Brescia, Brescia, Italy*
[134] *Variable Energy Cyclotron Centre, Homi Bhabha National Institute, Kolkata, India*
[135] *Warsaw University of Technology, Warsaw, Poland*
[136] *Wayne State University, Detroit, Michigan, USA*
[137] *Yale University, New Haven, Connecticut, USA*
[138] *Yonsei University, Seoul, Republic of Korea*
[139] *Zentrum für Technologie und Transfer (ZTT), Worms, Germany*
[140] *Affiliated with an institute formerly covered by a cooperation agreement with CERN*
[141] *Affiliated with an international laboratory covered by a cooperation agreement with CERN*

[a] Deceased.
[b] Also at Max-Planck-Institut fur Physik, Munich, Germany.
[c] Also at Italian National Agency for New Technologies, Energy and Sustainable Economic Development (ENEA), Bologna, Italy.
[d] Also at Dipartimento DET del Politecnico di Torino, Turin, Italy.
[e] Also at Lehigh University, USA.
[f] Also at Department of Applied Physics, Aligarh Muslim University, Aligarh, India.
[g] Also at Institute of Theoretical Physics, University of Wroclaw, Poland.